Correcting MAGIC Telescope data taken under non-optimal atmospheric conditions with an elastic LIDAR

Felix Schmuckermaier[1], Markus Gaug[2], Christian Fruck[1], Alexander Hahn[1], Victor Acciari[3], Jürgen Besenrieder[1], Dijana Dominis Prester[4], Daniela Dorner[5], David Fink[1], Lluís Font[2], Saša Mićanović[4], Razmik Mirzoyan[1], Dominik Müller[1], Lovro Pavletić[4], and Martin Will[1]

[1]Max-Planck-Institut für Physik, 80805 München, Germany
[2]Departament de Física, Universitat Autònoma de Barcelona and CERES-IEEC, 08193 Bellaterra, Spain
[3]Institut de Física d'Altes Energies, 08193 Bellaterra, Spain
[4]University of Rijeka, Department of Physics, 51000 Rijeka, Croatia
[5]Universität Würzburg, D-97074 Würzburg, Germany

Abstract. The Major Atmospheric Gamma-ray Imaging Cherenkov (MAGIC) telescopes are a system of two Imaging Atmospheric Cherenkov Telescopes (IACTs). IACTs make calorimetric use of the Earth's atmosphere, which allows them to reach large effective areas, but also makes them strongly dependent on the quality of the atmosphere at the time of the observations. Dust intrusions or clouds obscuring the observed Cherenkov light can then lead to a wrong reconstruction of the gamma-ray data. In order to mitigate this problem, the MPP group built and has been operating a single wavelength elastic LIDAR (LIght Detection And Ranging) system to perform real time ranged-resolved measurements of the aerosol transmission. This information is then used to quantify the quality of the telescope data, as well as to correct the data taken under suboptimal aerosol conditions. In this talk, the correction of atmospherically impaired IACT data will be described and the first systematic evaluation of the correction capabilities of the LIDAR system will be presented. The results describe the impact of the LIDAR corrections for a variety of atmospheric and observational conditions, and therefore contribute to a better understanding of the telescope's performance and related systematic uncertainties.

1. Introduction

The MAGIC telescopes consist of two IACTs (MAGIC I and MAGIC II) located at the Observatorio del Roque de los Muchachos (28.76°N 17.89°W, 2200 m a.s.l.) on the Canary Island of La Palma. Stereoscopic observations started in 2009, allowing detection of gamma rays with energies from around 50 GeV up to 100 TeV [1; 2]. IACTs make calorimetric use of the Earth's atmosphere, which allows these instruments to reach effective areas of the order of km^2, but also makes them strongly dependent on the quality of the atmosphere at the time of the observations. Changes in the aerosol conditions due to clouds or dust can affect the shape and brightness of the shower images detected in the telescope cameras, which ultimately can

lead to wrong reconstruction of the gamma-ray data. In order to mitigate this problem, the MAGIC collaboration has been operating a single wavelength elastic LIDAR (LIght Detection And Ranging) system, located next to the MAGIC telescopes, to perform real time ranged-resolved measurements of the atmospheric transmission. This information is then used to quantify the quality of the telescope data, as well as to correct the data taken under sub-optimal aerosol conditions.

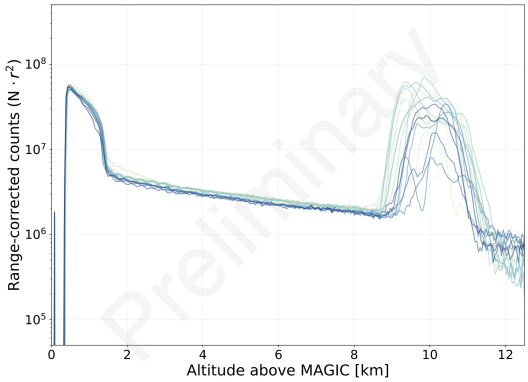

Figure 1. Range-corrected photo-electron count taken on November 13, 2015, revealing a higher aerosol content above the ground up to around 1.5 km as well as a layer of clouds between 8.5 km and 11 km above MAGIC.

2. Data Corrections using the Atmospheric Transmission Profile

2.1. Obtaining the LIDAR transmission profiles

The LIDAR initially provides a profile of the photo-electron counts. Figure 1 shows some examples of the range-corrected profiles as a function of altitude. Using the signal-inversion algorithm described in [3] the aerosol extinction profile, $\alpha_{\mathrm{LIDAR}}(r)$, can be extracted for the 532 nm laser wavelength. These profiles are then corrected for the fact that the wavelength spectrum of detected Cherenkov light is not centered at the LIDAR wavelength, but instead shows a strong contribution of UV light, centered at 400 nm.

The MAGIC LIDAR precedes the observed field-of-view of the MAGIC Telescopes with an angular offset of $\sim 5°$. Aerosol extinction profiles, $\alpha_{\mathrm{aer}}(r)$, are then evaluated as a function of range, r, and converted to integrated aerosol transmissions:

$$\tau_{\mathrm{aer}}(r) = \exp\left(-\int_0^r \alpha_{\mathrm{aer}}(r')\, r'\right) \equiv \tau_{\mathrm{aer}}(h) = \exp\left(-\int_0^{h/\cos\theta} \alpha_{\mathrm{aer}}(h')/\cos\theta\, h'\right) \quad , \qquad (1)$$

where θ is the LIDAR pointing zenith angle.

The aerosol transmissions, $\tau_{\mathrm{aer}}(h)$, are then divided into equidistant altitude, h, bins of 250 m bin width. Each altitude bin gets then interpolated in time. For observation periods up to 15 minutes outside the time range covered by LIDAR, the transmission profiles get extrapolated in time. In this way, an aerosol transmission profile can be attributed to each individual MAGIC science data event. Figure 2 shows example transmission profiles resulting from the atmospheric conditions portrayed in figure 1.

2.2. Energy correction

In first order approximation, the amount of Cherenkov light that reaches the IACT, for a given impact parameter, scales linearly with the gamma-ray energy [4]. This means that the relative energy bias, introduced by aerosol extinction, can be assumed proportional to τ_{aer}.

Normally, and particularly in case of cloud layers, different parts of the Cherenkov light

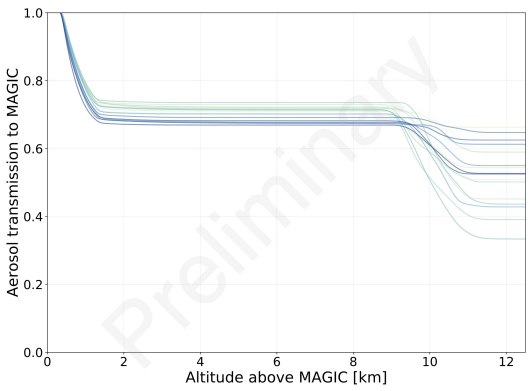

Figure 2. Integrated atmospheric transmission indicating a transmission at 9 km of around 0.7 during the night of November 13, 2015.

emitting particle shower lie within, above, or below the attenuating layer of particulates. For layers of low and moderate optical depth, it is sufficient [5] to simply scale the reconstructed shower energy with the average transmission seen by the Cherenkov light emitted along the shower:

$$\overline{\tau}_{\mathrm{aer}} = \int_0^\infty \epsilon(h) \cdot \tau_{\mathrm{aer}}(h)\ \mathrm{d}h \quad . \tag{2}$$

The normalized emission profile of observable Cherenkov light from each shower, $\epsilon(r)$, is estimated using the respective reconstructed altitudes of each shower maximum [1; 6], obtained from stereo reconstruction, and an energy-dependent, Gaussian, longitudinal extension of width σ, which has been obtained from toy MC air-shower simulations.

The new energy estimation E_{corr} is obtained by scaling the old estimate E_{est} with the inverse of the average optical depth:

$$E_{\mathrm{corr}} = \frac{E_{\mathrm{est}}}{\overline{\tau}_{\mathrm{aer}}}\,. \tag{3}$$

Since the reconstructed energy appears in the width of the longitudinal profile, this process is iterated until convergence is reached.

2.3. Instrument response function correction

Up-scaling the energy of each air shower event alone is not sufficient for a retrieval of the correct energy spectrum, because the instrument response functions of MAGIC also show a strong dependence on energy [1]. Therefore, the correction of the energy spectrum is implemented with a bin-wise correction of the effective collection areas and energy migration functions of the system. In this approach, we explicitly assume that the cut-efficiencies, which themselves depend on the distributions of the Hillas parameters [4; 6; 7], are not altered by the presence of aerosols, an assumption that is only approximately true for not too large values of τ_{aer} [8].

We make an elapsed-time-weighted histogram of the event-wise correction factors. The histogram represents for how long has the atmosphere been in conditions in which the energy correction factor (averaged for gamma-like events of all energies) had a given value. This is done in bins of zenith angle θ, hence we have t_{elapsed} in bins of $\overline{\tau}_{\mathrm{aer}}$ and θ. Then we can obtain the average corrected effective area for a given zenith angle as:

$$\langle A_{\mathrm{eff}}(E_{\mathrm{true}}, \theta)\rangle = \frac{\sum_i A_{\mathrm{eff}}(E_{\mathrm{true}} \cdot \overline{\tau}_{\mathrm{aer,i}}) \cdot t_{\mathrm{elapsed,i}}(\theta)}{\sum_i t_{elapsed,i}(\theta)} \tag{4}$$

where the sum is over the bins of $\overline{\tau}_{\mathrm{aer}}$. This is therefore the average of energy-shifted effective areas, weighted with the time spent in each observation condition. The use of the elapsed time (instead of effective time) simplifies the calculation, and makes no actual difference given that dead time fraction is of around 1% and similar for all data. Finally, averaging in zenith bins provides the average effective area for the whole sample.

3. Evaluation of the performance of the LIDAR-based corrections

3.1. Data set

In this work, Crab Nebula data from mid 2013 until early 2020 is analyzed, covering a time period of almost seven years. The Crab Nebula is observable by MAGIC only from September until April. The data set contains observations taken at zenith angles between 5° and 62°. At higher zeniths, it becomes increasingly challenging for the LIDAR to reach the necessary heights with its limited range, which makes an alternative measurement of the atmospheric extinction necessary [9]. Due to the very different systematics involved, we have decided not to include those "very large zenith angle" data sets. Furthermore, only data taken under *dark* conditions have been used, requiring a low level of night sky background [10].

The data were then classified according to aerosol transmission from 9 km above ground, $T_{9\,\mathrm{km}}$. The maximum emission of Cherenkov light of atmospheric air showers for 100 GeV gamma-rays is reached at a height of close to 9 km [11]. The Crab Nebula data were then divided into four groups: A low transmission region ($0.5 < T_{9\,km} < 0.65$), a medium transmission region ($0.65 < T_{9\,km} < 0.82$), a high transmission region ($0.82 < T_{9\,km} < 0.9$) and lastly a region with only data of the best possible quality ($T_{9\,km} > 0.95$). In total, about 176 hours of data with $T_{9\,km}$ above 0.95 have been used, 26 hours in the high transmission range, 16 hours in the medium and 10 hours in the low transmission range.

3.2. Construction of the reference spectrum

In order to quantify improvements to the spectra taken under non-optimal conditions, a reference spectrum, which serves as the standard for comparison, needs to be defined. The reference spectrum has been built from the best possible data with $T_{9\,\mathrm{km}} > 0.95$ only. For the following results, only a single spectrum is used, for which all the available data is combined. The spectra is obtained by fitting the data with a log-parabola function:

$$\frac{\mathrm{d}\phi}{\mathrm{d}E} = f \cdot \left(\frac{E}{275\,\mathrm{GeV}}\right)^{a - b^2 \cdot \log_{10}\left(\frac{E}{275\,\mathrm{GeV}}\right)} \tag{5}$$

The same spectral fit will also be used for the data taken under non-optimal atmospheric conditions.

3.3. Evaluation of the LIDAR performance

Figure 3 shows the uncorrected and corrected SED taken in the night previously used for the example photo-electron and transmission profiles (November 13, 2015), where $T_{9\,\mathrm{km}}$ showed values of around 0.7. The reference spectrum is given by the dashed spectrum in dark green. After applying corrections, a good agreement of the corrected spectrum with the reference can be seen for this night.

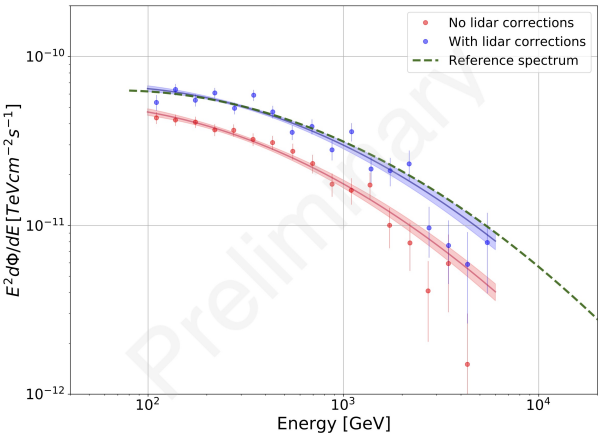

Figure 3. Example spectrum from November 13, 2015, showing the impact of the LIDAR corrections on data in the 0.65 to 0.82 transmission bin without LIDAR corrections (red) and in with corrections (blue). The corresponding reference spectrum is shown in green.

In order to further investigate the influence of the zenith angle, under which the data was taken, the data have been further classified into three zenith bins: A low zenith bin from 5° to 35°, a mid zenith bin from 35° to 50° and a high zenith bin from 50° to 62°.

Since individual nights can show limited statistics, one can combine all available nights from a certain transmission and zenith bin into a single spectrum, to systematically evaluate the effect of the corrections. Figure 4 portrays the resulting spectra. A three by three arrangement covers all combinations of aerosol transmission and zenith angle bins. The transmission and zenith angle region is given in the subplot titles. An individual subplot contains the resulting SED before and after applying the LIDAR corrections shown together with the reference spectrum. The effective observation time of the corrected and uncorrected data is shown in the top right of each subplot.

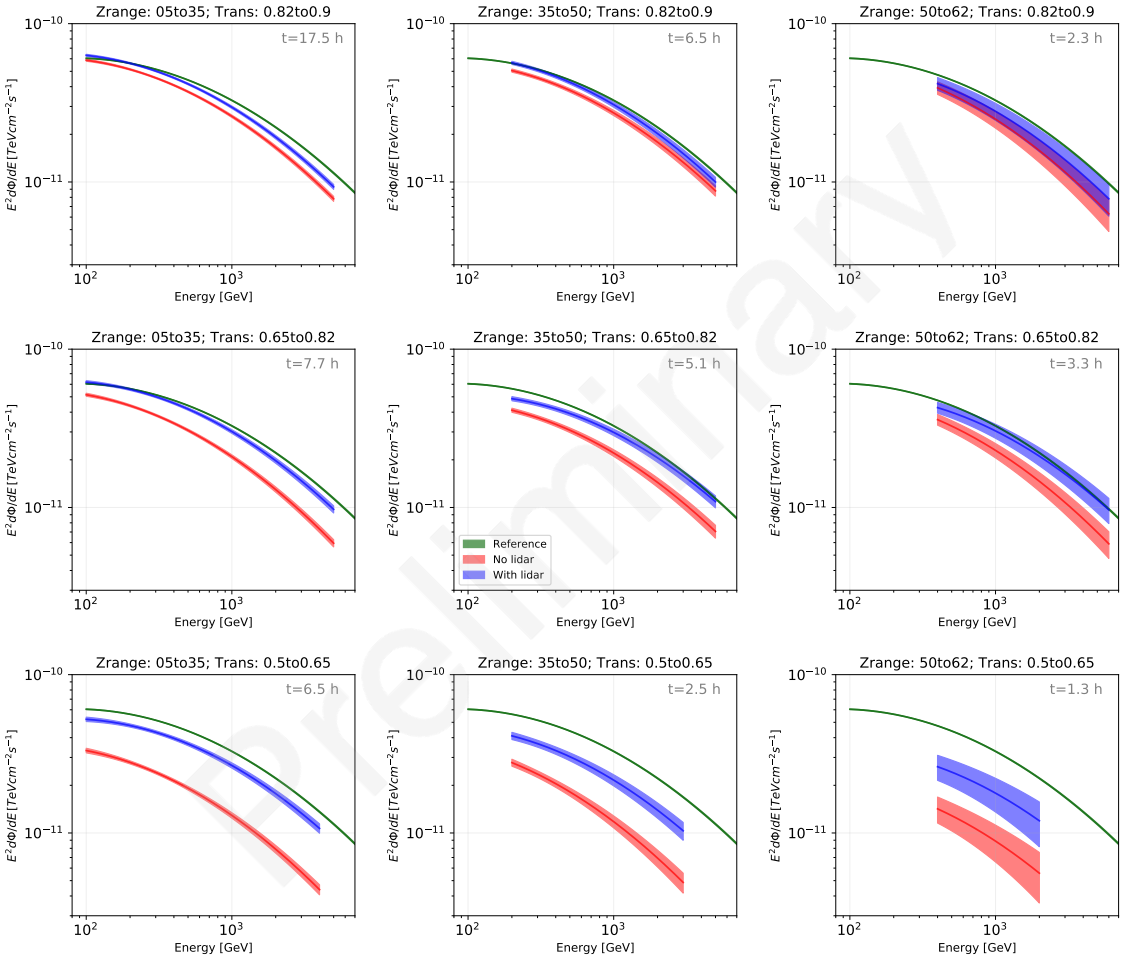

Figure 4. Overall spectral fits for nine different zenith angle and aerosol transmission bins without (red) and with (blue) LIDAR corrections. The reference spectrum is given in green. The effective time of the data used for the individual spectra is given in the top right corner of each subplot.

In the top row, results for the highest transmission bin are portrayed. The spectra show only small offsets from the reference without using LIDAR corrections. Using the corrections, an agreement better than 15% (maximum deviation) is achieved for all zenith angles.

For medium transmissions, the uncorrected spectra can show deviations up to 50%. The spectra achieve an agreement up to 15% with the reference for all zeniths after applying LIDAR corrections.

For the lowest transmission, the limitations of the method become apparent. For low zeniths, the spectrum gets up-scaled by over 30% but still shows some remaining deviation from the reference by around 20%. For medium zeniths, a strong correction is also achieved, but deviations from 25-40% to the reference prevail. In the highest transmission regime only very little data is available. Again, a strong correction can be seen but the results are not sufficient for regular usage of the data.

4. Conclusion

An elastic LIDAR serves as the main atmospheric monitoring instrument for the MAGIC telescopes. In addition to characterizing the atmospheric conditions for the application of quality cuts, the obtained aerosol extinction profiles can be used to correct MAGIC science data collected under non-optimal aerosol conditions. We have presented a method for the correction of the energy of individual gamma-ray events, as well as the instrument response function. We evaluated the performance of LIDAR-based corrections under different aerosol conditions and zenith angles by comparing spectral fits of almost seven years of Crab data. The results allow for a better estimation as well as a reduction of the systematic uncertainties of IACTs under sub-optimal aerosol conditions.

Acknowledgments

This work would have been impossible without the support of our colleagues from the MAGIC collaboration. We are especially grateful to the many shifters who have helped to debug and improve the LIDAR system. We would also like to thank the Instituto de Astrofísica de Canarias for the excellent working conditions at the Observatorio del Roque de los Muchachos in La Palma.

The financial support of the Spanish grant PID2019-107847RB-C42, funded by MCIN/AEI/ 10.13039/501100011033, the German BMBF and MPG, and by the Croatian Science Foundation (HrZZ) Project IP-2016-06-9782 and the University of Rijeka Project uniri-prirod-18-48 is gratefully acknowledged.

References

[1] Aleksić J *et al.* 2016 *Astroparticle Physics* **72** 76–94 (*Preprint* 1409.5594)

[2] MAGIC Collaboration *et al.* 2020 *Astronomy & Astrophysics* **635** A158 (*Preprint* 2001.09566)

[3] Fruck C, Gaug M, Hahn A *et al.* 2022 *MNRAS* **15**(3) 4520–4550 (*Preprint* arXiv:2202.09561)

[4] Hillas A 1985 *Proc. of the* 19$^{\text{th}}$ *International Cosmic Ray Conference, La Jolla* pp 445–448

[5] Garrido D, Gaug M, Doro M, Font L, López-Oramas A and Moralejo A 2013 *Proceedings of the 33*$^{\text{rd}}$ *ICRC, Rio de Janeiro* p 0465 arXiv:1308.0473

[6] Fegan D J 1997 *Journal of Physics G: Nuclear and Particle Physics* **23** 1013–1060 URL https://doi.org/10.1088/0954-3899/23/9/004

[7] Aliu E *et al.* 2009 *Astroparticle Physics* **30** 293–305 (*Preprint* 0810.3568)

[8] Sobczyńska D, Adamczyk K, Sitarek J and Szanecki M 2020 *Astroparticle Physics* 102450 URL http://www.sciencedirect.com/science/article/pii/S0927650520300232

[9] Mirzoyan R, Vovk I, Peresano M, Temnikov P, Zaric D, Godinovic N, van Scherpenberg J, Besenrieder J, Teshima M and MAGIC Very Large Zenith Angle Observation Working Group 2020 *Nuclear Instruments and Methods in Physics Research A* **952** 161587 (*Preprint* 1903.04989)

[10] Pavletic L *et al.* 2022 *AtmoHEAD 2022, Anacapri* these proceedings

[11] Bernlöhr K 2000 *Astroparticle Physics* **12** 255–268 (*Preprint* astro-ph/9908093)